Journal of The Electrochemical Society, **153** (10) A1992-A1997 (2006)
0013-4651/2006/153(10)/A1992/6/$20.00 © The Electrochemical Society

Stability Improvement of $LiMn_2O_4$ Thin-Film Cathodes under High Rate and Over-Discharge Cycling

K.-F. Chiu,[a,*,z] H. C. Lin,[b] K. M. Lin,[a] and C. C. Chen[a]

[a]*Department of Materials Science and Engineering, Feng Chia University, Taichung, Taiwan*
[b]*Department of Materials Science and Engineering, National Taiwan University, Taipei, Taiwan*

Thin films of spinel lithium manganese oxides were prepared by sol-gel method. The annealing time and temperatures were optimized to obtain crystalline $LiMn_2O_4$ thin films. The as-synthesized films were coated with a thin layer of alumina or lithium phosphorus oxynitride (LiPON) by radio frequency sputtering. The coatings were amorphous as characterized by X-ray diffraction. The electrochemical properties of the coated and uncoated thin-film cathodes were characterized and compared. The cells made of the lithium manganese oxide cathodes were discharged at different rates. At higher discharge rates, both the alumina and the LiPON-coated samples exhibited higher discharge potential plateaus than the uncoated spinel. As the cells were cycled in a wide voltage window of 4.0–1.5 V, the coated cathodes exhibited less capacity fading. For samples immersed in acid solution before cycling, the surface-coated samples showed greater stability.
[DOI: 10.1149/1.2266531]

Manuscript submitted April 10, 2006; revised manuscript received June 12, 2006. Available electronically August 29, 2006.

The spinel $LiMn_2O_4$, due to its lower cost and environmental friendliness,[1-3] has been viewed as an alternative choice for layered $LiCoO_2$ cathodes. However, the $LiMn_2O_4$ cathode materials exhibit some stability issues, among which the capacity fading during cycling is commonly observed,[4-8] especially during cycling or storage at 55°C. An important factor for the capacity fading is the manganese dissolution,[5] which may be induced by the formation of acid resulting from reaction of residual H_2O with electrolyte. The presence of acid in the electrolyte contributes to the disproportion reaction of unstable Mn^{3+} to Mn^{2+} and Mn^{4+}, and the Mn^{2+} can readily dissolve. The resulted compounds, containing mostly Mn^{4+}, have lower capacity. The reaction may be further enhanced by elevated temperature. In addition, Cho and Thackeray[5] showed that capacity fading is associated with the structural changes of spinel at the end of discharge. The recent study of Lee et al.[4] proposed that, as the $LiMn_2O_4$ cathode was cycled to a voltage less than 3.0 V, large capacity fading occurred. The deep discharge reduced the average oxidation state of manganese from 3.5 to 3, which led to a sufficiently large cubic-tetragonal structural change to destroy the structural integrity and increase the possibility of manganese dissolution.

Currently, the main approaches applied to suppress the capacity fading are substituting Mn^{3+} ions with other cations,[8,9] or coating the $LiMn_2O_4$ particle surface by a protective layer using solutions containing precursors of metal oxides.[10-13] However, the materials resulting from these approaches were in powder form, which generally requires binders and carbon black to fabricate electrodes for test cells. Therefore, other factors such as binder or solvent degradation or decomposition cannot be ruled out. In addition, the solution method involved firing the oxide solution gel with $LiMn_2O_4$ powders, and may result in the formation of solid solutions at the powder surface, which further complicates the factors of capacity fading-retention.

In the present study, $LiMn_2O_4$ thin films 1–2 μm thick are synthesized by sol-gel method and deposited on the substrates, which does not require the usage of binders and carbon black. An oxide layer is coated on the film surface by sputter deposition, and there are no chemical reactions between the coatings and $LiMn_2O_4$. The minimum coating thickness can also be controlled precisely by sputter deposition. The surface-coated films were tested by high rate discharge, deep discharge cycles, and acid treatments. The enhanced stability by the surface coatings is verified.

Experimental

Li-Mn-O thin films were prepared by the sol-gel method using lithium acelacetonate, $LiC_2H_7O_2$, and manganese acelacetonate, $Mn(CH_3COCHCOCH_3)_2$, as precursors (purchased from Johnson Matthey).[2] The solvents were 1-butanol (from Nippon Chemical), water, and acetic acid (from Acros). The precursors and solvents were mixed and stirred at 250°C. Suitable amount of water was added during the process to maintain the pH level. Heating and stirring continued until a red-brownish gel was obtained. By adding suitable amount of water at elevated temperature, the above process took only ~30 min to finalize. The gel was then filtered by a 0.2 μm filter, and spin coated[2] on stainless steel foils. The area of the stainless steel substrate is 1.33 cm^2. The plated thin film was then dried at 300°C. The process was repeated 5–10 times to obtain a film weighted at 2.0 mg (measured by a Sartorius CP2250 microbalance) with an uncertainty of 0.1 mg. The dried precursor thin films were fired at 600–800°C in air using an electric furnace to obtain $LiMn_2O_4$ thin films.

A thin layer of alumina or lithium phosphorus oxynitride (LiPON) was sputter deposited on the $LiMn_2O_4$ films in a water-cooled vacuum chamber (base pressure $\sim 10^{-6}$ mbar). The LiPON films were deposited from a 2 in. diameter Li_3PO_4 target (purchased from Superconducting Components Inc.) with 80 W sputter gun power in pure N_2 gas (99.9%) of 20 mTorr, and the target-substrate distance was 70 mm. The alumina films were deposited using a 2 in. Al_2O_3 target (purchased from Superconducting Components Inc.) with gun power of 100 W and pressure of 20 mTorr (99.9% pure Ar). The thickness of the alumina and LiPON coatings was kept at ~130 nm by controlling the thickness deposition rates and deposition time. The deposition rates were ~2.1 and ~4.3 nm/min, and the deposition times were ~63 and ~30 min for alumina and LiPON, respectively.

The crystallography of both coated and uncoated $LiMn_2O_4$ thin films was characterized using Cu Kα X-ray diffraction (XRD). The chemical composition of Li and Mn was measured by inductively coupled plasma atomic emission spectroscopy (ICP-AES, from Jarrel-Ash, ICAP 9000). The ICP-AES provided the quantitative chemical concentrations of measured elements ($\mu g\ L^{-1}$). The ICP-AES measurement limit is 10 $\mu g\ L^{-1}$ for Li and 5 $\mu g\ L^{-1}$ for Mn. The measured concentrations are typically more than 60 $\mu g\ L^{-1}$ for Li, and 600 $\mu g\ L^{-1}$ for Mn. The estimated error of the atomic ratios of Li/Mn is around 0.002. The ratios of O and Mn were determined by relative peak areas of O/Kα and Mn/Lα, obtained from energy dispersive X-ray spectroscopy (EDX). The data were collected and corrected according to ZAF factors by a software package provided by Horiba, U.K. The uncertainty of Mn/O ratios measured by EDX is around 13%; therefore, these ratios were only a qualitative index rather than precise compositions. The film surface morphology was observed by scanning electron microscopy (SEM, Jeol JSM-6700F).

The films deposited on stainless steel foils were packed in conventional coin cells (type 2032) with lithium foils as counter and

---

[*] Electrochemical Society Active Member.
[z] E-mail: kfchiu@fcu.edu.tw

Table I. The composition of precursor solution, as dried and annealed LiMn2O4 thin films.

Sample	Li (atom %)	Mn (atom %)	O (atom %)
Sol	1.06	2	
As-dried	1.06	2	3.6
600°C	1.10	2	3.3
800°C	1.04	2	3.3

reference electrodes. The electrolyte was 1 M $LiPF_6$/ethyl carbonate/ethyl methyl carbonate (EC-EMC) (1:2) solution. The coin cell packaging was carried out in Ar atmosphere. Charge-discharge and cycling tests were carried out using a Jiehan 5000 electrochemical measurement system. The coated and uncoated cells were cycled in the ranges of 3.0–4.3 V and 1.5–4.3 V. The cells were charged at constant current of 75 $\mu A\ cm^{-2}$ to 4.3 V, and then kept at constant potential until the current density drop below 1 $\mu A\ cm^{-2}$. Discharge current was 75 $\mu A/cm^2$. Discharge curves at different current densities of 75 $\mu A/cm^2$ to 7.5 mA/cm^2 were also compared. Some samples were deliberately immersed into 0.25 M H_2SO_4 for 1 min to demonstrate the different cycling stability of the coated and uncoated films.

Results and Discussion

The compositions of the sol-gel synthesized lithium manganese oxide films are shown in Table I. The Li/Mn and Mn/O ratios are approximately the same in the solution, as-dried precursor films, and annealed films. Figure 1 shows the XRD patterns of the 600°C annealed film on the stainless steel substrate, which exhibits a well-crystallized $LiMn_2O_4$ phase. The 800°C annealed film shows higher diffraction intensity, but a second phase also develops. Therefore, the following tests were carried out using the 600°C annealed $LiMn_2O_4$ thin films.

With oxide coatings, the crystallography of the $LiMn_2O_4$ films does not alter, but shows lightly lower diffraction intensity. The thin coatings are over the XRD detection limits and no crystalline phases related to the oxide coatings can be detected. Figure 2a-c is the SEM micrograph (secondary electron imaging) of the uncoated and coated $LiMn_2O_4$ films. All the films are similar and exhibit very rough and porous surface morphologies. Considering the large thickness variation of the order of ~μm, the coatings of 130 nm may not fully cover the surface. In order to distinguish these two types of samples, they are referred to as alumina and LiPON coated in the following text.

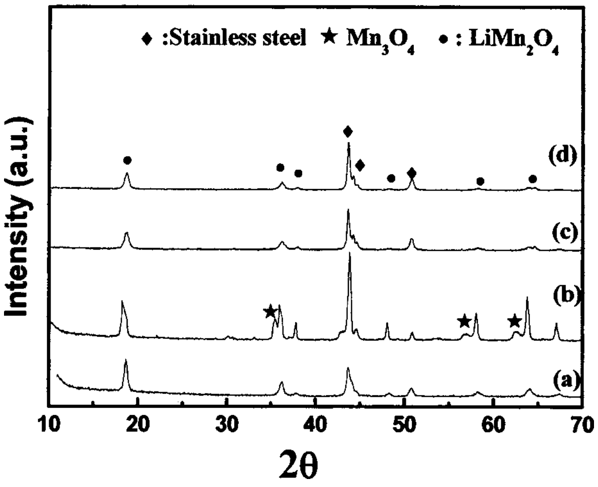

Figure 1. XRD patterns of uncoated lithium manganese oxide thin films annealed at (a) 600°C and (b) 800°C, and the 600°C annealed films coated with (c) alumina and (d) LiPON layers.

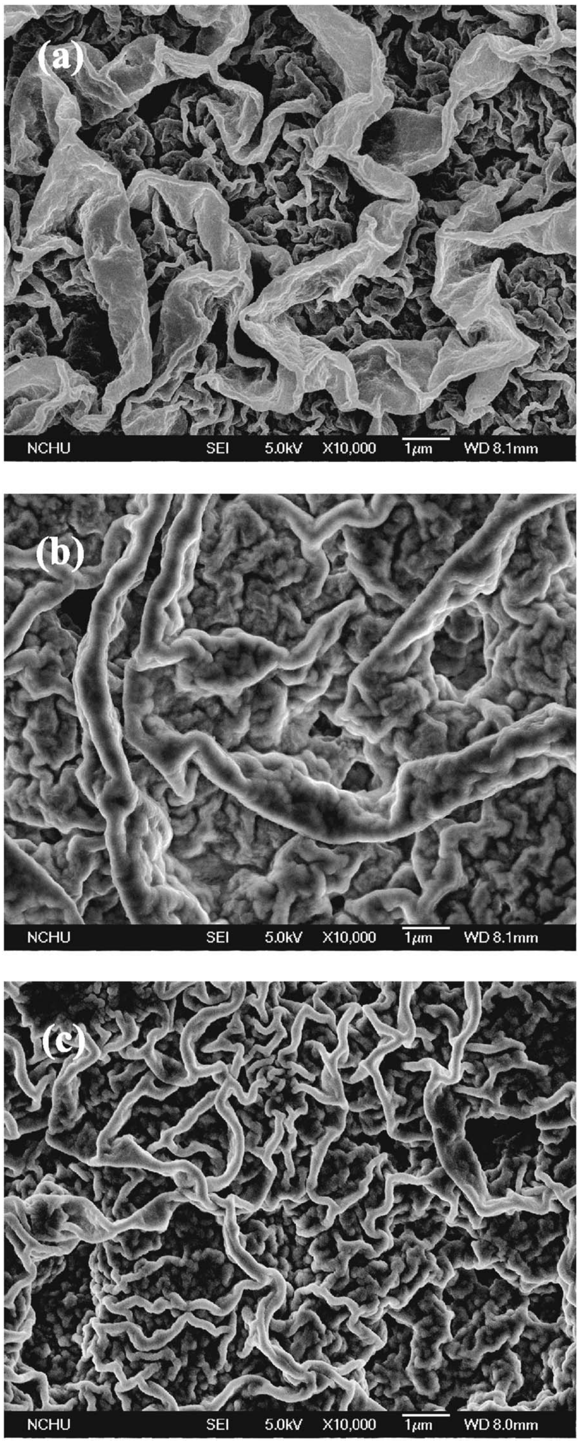

Figure 2. SEM micrographs of (a) uncoated, (b) alumina-coated, and (c) LiPON-coated $LiMn_2O_4$ thin-film cathodes.

The initial discharge curves of the coated and uncoated films as a function of discharge rates were measured to compare the capacity retention of different samples. Discharge current densities were set at 75 $\mu A/cm^2$, 750 $\mu A/cm^2$, and 7.5 mA/cm^2, which corresponded to 0.45, 4.5, and 45 C. As shown in Fig. 3a-c, at low discharge rates

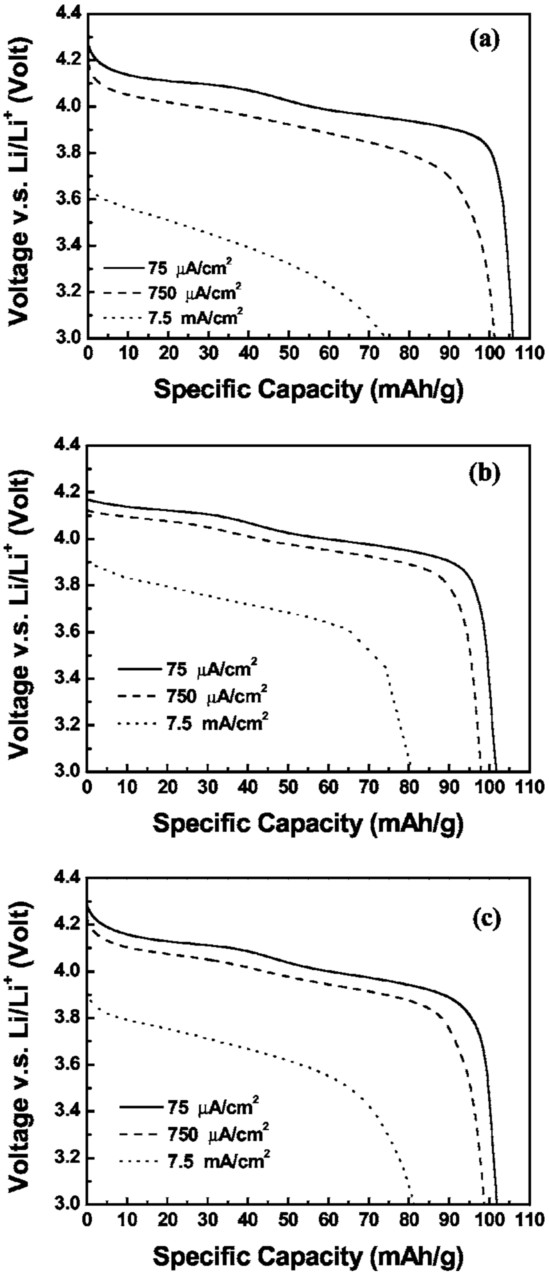

Figure 3. Discharge curves of the (a) uncoated, (b) alumina-coated, and (c) LiPON-coated $LiMn_2O_4$ thin-film cathodes under different discharge currents.

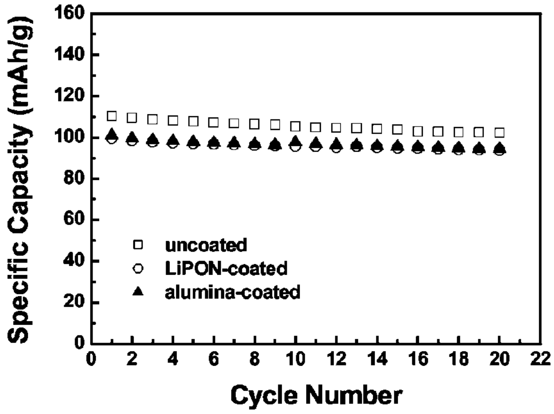

Figure 4. Capacities as a function of cycle number for coated and uncoated $LiMn_2O_4$ thin-film cathodes cycled within 4.3–3.0 V.

the coated and uncoated samples both exhibit similar discharge curves with clear 4.1 and 3.9 V plateaus, except that the coated samples show slightly lower capacities.

As the discharge rates increase, the potential plateaus and capacities decrease. For the uncoated $LiMn_2O_4$ films, the curve exhibits a greater slope at the high discharge rate (7.5 mA/cm^2), and no obvious plateau above 3.6 V can be recorded. On the other hand, both the alumina and LiPON coated films exhibit a plateau at 3.9 to 3.6 V region, as discharge at the same rate. The alumina-coated sample shows best performance, and still retains a capacity of around 70 mAh/g at 3.6 V. The results indicate that the surface oxide coating is effective in improving the stability of $LiMn_2O_4$ films under high rate discharge.

The decrease of discharge voltage and useful capacity is due to the cell resistance, which is mostly contributed by the lithium ion transportation into and through the cathode film. From this point of view, the oxide-coated samples have higher resistance and are supposed to have lower voltage and capacity under high rate discharge. However, both the alumina and LiPON-coated samples exhibit higher voltage and capacity. It may be that under high rate discharge a large lithium ion flux is inserted into the surface of cathode in a very short period, whereas ion transportation in the solid cathode film is slow. It results in polarization, as the near-surface $LiMn_2O_4$ lattices are overdischarged, and those at the bottom of the film are left unreacted. In these overdischarged lattices, the average oxidation state of manganese decreases, which leads to structural changes, manganese dissolution, and deteriorates the film integrity. For the alumina and LiPON-coated films, the coatings provide an extra support on the films surface, which improves the structural integrity. The coatings also limit the manganese dissolution. As a result, the coated cells show higher discharge voltage and capacity. The results are similar to the study of Dudney[14] on LiPON-coated $Li_xMn_{2-y}O_4$ thin-film cathode, where the coated sample maintains higher discharge capacity and potential (>3.0 V) compared with bare sample as the discharge currents increase from 2 to 40 $\mu A\ cm^{-2}$. It was proposed that for the bare sample, the corrosion layer (due to Mn dissolution) at the cathode/liquid electrolyte interface increases the internal cell resistance and therefore reduces the discharge potential.[14]

Figure 4 shows the capacity as a function of cycle number for the coated and uncoated $LiMn_2O_4$ thin films cycled within 4.3–3.0 V range at discharge current of 75 $\mu A/cm^2$. The coated samples show only slightly lower capacity because some area of the film surface is covered with inactive oxide coating. After 20 cycles, all films exhibit similar capacity fading behaviors. The LiPON-coated $LiMn_2O_4$ cathode shows a capacity fading of around 6%, which is more stable compared with the reported results of LiPON-coated $Li_xMn_{2-y}O_4$ thin-film cathodes.[14] It is because our sol-gel synthesized samples are well crystallized. As for the alumina-coated cathode, it exhibits a capacity fading of ~6.5%, which is comparable with published data.[11,13]

The results of Kim et al.[13] showed that alumina-coated sample actually exhibits greater capacity fading than the uncoated one as cycled at 50°C, and it was proposed that Al^{3+} may react with $LiMn_2O_4$ during colloidal coating process at 400°C. In fact, surface coatings using precursor solution or colloidal suspension methods generally required postdeposition annealing,[10-13] which may result in formation of solid solutions on the surface of the cathode materials. For instance, the Al_2O_3, SiO_2, and $LiCoO_2$ coatings all showed a certain degree of interface reactions with the cathode materials.[10,13] Therefore, the changes of cycling performance may be attributed to both the surface coatings and the solid solutions, formed by reactions between coatings and cathode materials. In our

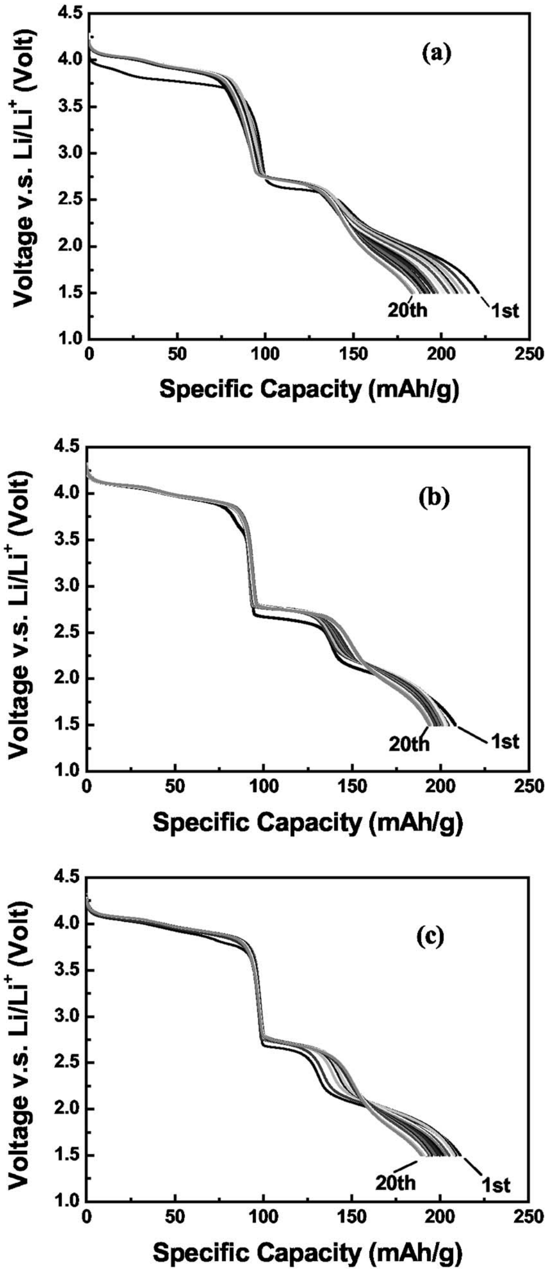

Figure 5. Discharge curves of (a) uncoated, (b) alumina-coated, and (c) LiPON-coated $LiMn_2O_4$ thin-film cathodes cycled within 4.3–1.5 V.

Table II. Discharge capacity (mAh/g) and percentage of capacity fading in 4.3–1.5 V cycling window and different voltage ranges for the uncoated and coated $LiMn_2O_4$ thin films.

Samples/voltage ranges	Cycle 1	Cycle 2	Cycle 20	Fading $[(C_{20} - C_1)/C_1]$
Uncoated				
4.3–3.0 V	98	97	92	−6%
3.0–2.5 V	43	44	44	~0%
2.5–1.5 V	80	75	47	−41%
4.3–1.5 V	221	216	183	−17%
Alumina-coated				
4.3–3.0 V	94	94	95	~0%
3.0–2.5 V	46	48	54	18% (increase)
2.5–1.5 V	67	63	40	−40%
4.3–1.5 V	207	204	189	−9%
LiPON-coated				
4.3–3.0 V	98	97	98	~0%
3.0–2.5 V	29	33.3	45	54% (increase)
2.5–1.5 V	84	78	47	−44%
4.3–1.5 V	211	209	190	−10%

study the sputter deposition and electrochemical tests were carried out at room temperature; therefore, the reactions between the coatings and the $LiMn_2O_4$ cathodes may be negligible.

As the cycling range expands to 4.3–1.5 V, the coated and uncoated films clearly show different cycling stability (Fig. 5a-c). The capacity values are shown in Table II. For the uncoated sample, although a higher initial discharge capacity is recorded, the capacity fading after 20 cycles is as much as 17%. Both the alumina and LiPON-coated films exhibit better stability with capacity fading of around 10%. At the end of 20 cycles, the coated samples show higher capacity than the uncoated one. The more significant capacity fading under wider cycling range (4.3–1.5 V) can be attributed to the overdischarge-induced manganese dissolution and structural deterioration, as well documented.[4-13] The structural change from cubic $Li_{1-x}Mn_2O_4$ to tetragonal $Li_{1+x}Mn_2O_4$ occurs below 3.0 V. Further discharge results in tetragonal $Li_2Mn_2O_4$, where disproportion of unstable Mn^{3+} into Mn^{4+} and Mn^{2+} renders the manganese dissolution.[5,7] The oxide coatings reduce the active surface area and lower the possibility of manganese dissolution. In addition, the oxide coatings provide a capping effect. The coated films therefore may endure the large stress caused by the cubic-tetragonal structural change as discharged below 3.0 V. Note that, as the cycling number increases, the oxide-coated samples seem to gradually develop larger potential plateaus within 3.0–2.5 V range (Fig. 5b and c).

The 3.0–2.5 V potential corresponds to the insertion of excess Li ions into the original nonactive octahedral sites in cathodes, i.e., $Li_{1+x}Mn_2O_4$. However, at $x = 1$, the $Li_2Mn_2O_4$ tetragonal phase is generally unstable and Mn dissolution occurs, leading to the decrease of capacity. Therefore, for the uncoated sample, the increase of 3.0–2.5 V plateau is not significant, and total capacity decreases more rapidly. For the oxide-coated samples, the Mn dissolution is suppressed. In addition, the coatings reduce active area on the cathode surface, which limits the diffusion of the excess Li ions into film body at initial cycles. After more cycles, the films become fully active and therefore the larger potential plateaus gradually develop.

In order to study the phenomenon, the capacities at different potential regions (4.3–3.0 V, 3.0–2.5 V, and 2.5–1.5 V) as a function of cycling number are shown in Fig. 6a-c, and the detail capacity values between cycles 1 and 20 for different voltage ranges are also shown in Table II. The initial capacity of uncoated films at 4.3–3.0 V range is ~98 mAh/g, which is lower than the typical value of ~120 mAh/g for $LiMn_2O_4$. It may be due to the lack of conductive additives, carbon black, or graphite, which are not applied in this study. At 2.5–1.5 V range, the films are severely overdischarged, and all films show obvious capacity fading of 40–44%. Interestingly, at 3.0–2.5 V range the capacity of uncoated films stays almost unchanged, whereas the alumina and LiPON-coated films show significant increase of 18 and 54%, respectively. The results indicate that the oxide coatings may stabilize the tetragonal $Li_{1+x}Mn_2O_4$ phase, allowing more Li insertion. At $x = 1$, the $Li_2Mn_2O_4$ tetragonal phase is unstable and Mn dissolution occurs, and the capacity decreases. The oxide coatings suppress the Mn dissolution and thus stabilize the tetragonal phase. As mentioned in the previous section, after more cycles the cathodes become fully active and the larger potential plateaus develop, corresponding to the increased 3.0–2.5 V plateau in Fig. 5b, 5c, 6b, and c. As a consequence, the Mn^{3+}/Mn^{2+} couple of the tetragonal phase can exist in the films and be reoxidized to Mn^{3+}/Mn^{4+} as the cells are charged, which somehow compensates the capacity fading. For the LiPON and alumina-coated films, the amounts of capacity fading at 4.3–3.0 V region are as low as 0 and 1%, respectively.

Because the manganese dissolution-induced capacity fading is

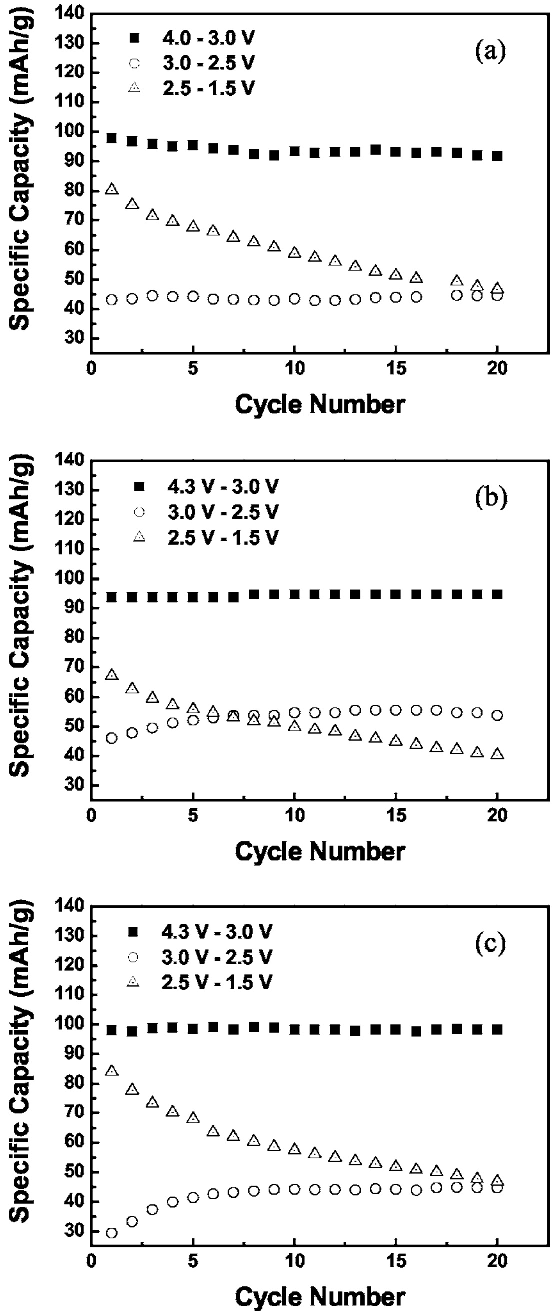

Figure 6. Discharge capacities at voltage ranges of 4.3–3.0 V, 3.0–2.5 V, and 2.5–1.5 V for (a) uncoated, (b) alumina-coated, and (c) LiPON-coated $LiMn_2O_4$ thin-film cathodes cycled within 4.3–1.5 V.

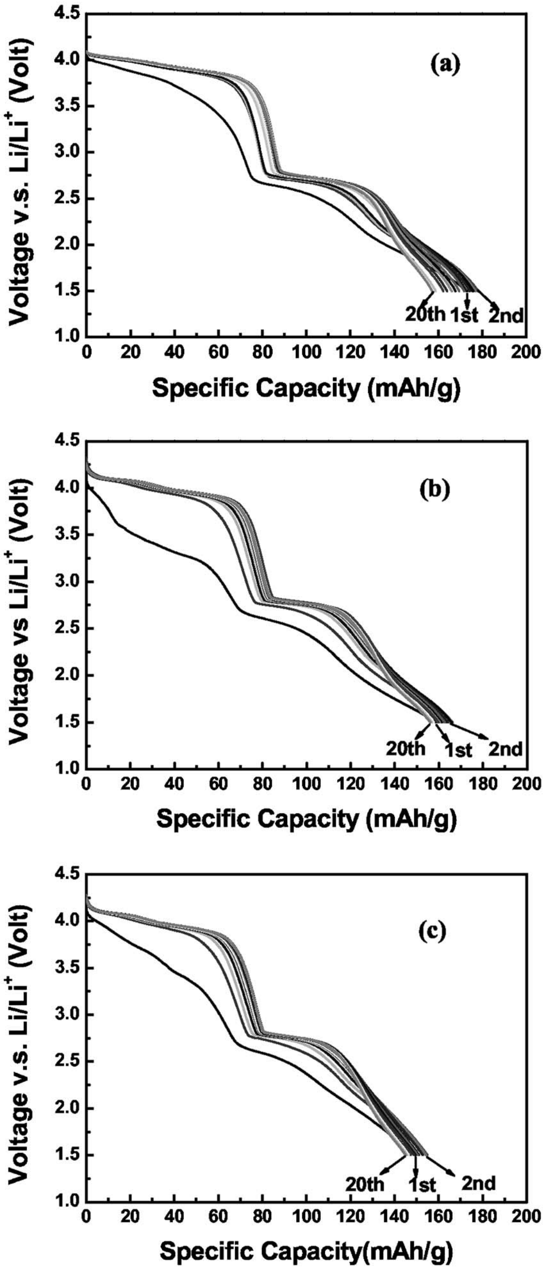

Figure 7. Discharge curves of (a) uncoated, (b) alumina-coated, and (c) LiPON-coated $LiMn_2O_4$ thin-film cathodes immersed in acid solution before cycled within 4.3–1.5 V.

often thought to associate with the acid formation due to the reaction between the residual water and electrolyte,[4-8] the coated and uncoated samples were deliberately treated in 0.25 M H_2SO_4 for 1 min, followed by cycling test. As shown in Fig. 7a-c, the acid treatment damages the films surface, and the initial discharge curves of all the samples show a great slope. However, in the second discharges the cell performances are back to normal condition. Again, the surface coatings effectively enhance the cycling stability. The capacity fading between cycles 1 and 20 is 9% for the uncoated sample, whereas only 2 and 3% are recorded for LiPON and alumina-coated samples. For the capacity fading between cycle 2 (recovered from sloppy cycle 1) and cycle 20, the uncoated sample shows 12% of fading and LiPON and alumina-coated samples show only 5 and 6%. Kim et al.[13] have suggested a HF scavenging mechanism, which enhances the cycling properties of ZrO_2-coated $LiMn_2O_4$ cathodes. They also mentioned that Al_2O_3 can also act as a HF scavenger. The alumina and LiPON coatings here may have similar function, which results in enhanced resistance to acid. The results have demonstrated that the oxide coatings are still effective even when being treated in such harsh environment as acid solution.

Conclusion

The cycling stability of sol-gel synthesized $LiMn_2O_4$ thin films has been investigated. The films coated with alumina and LiPON are shown to have improved stability under high rate and overdischarge cycles. At a discharge rate as high as 45 C (7.5 mAh/g), both of the alumina and LiPON-coated samples exhibited higher potential plateau and discharge capacity than the bare ones. As the cells were cycled in a wide voltage window of 4.3–1.5 V, the coated cathodes exhibited less capacity fading. Even for samples immersed in acid solution before cycling, the surface coated samples showed greater stability.

Acknowledgments

This research was sponsored by R.O.C. National Science Council under contract no. NSC 94-2216-E-035-007-, and by Feng Chia University under contract no. FCU94-GB-47.

Feng Chia University assisted in meeting the publication costs of this article.

References

1. X. Sun, X. Q. Yang, M. Balasubramanian, J. McBreen, Y. Xia, and T. Sakai, *J. Electrochem. Soc.*, **149**, A842 (2002).
2. Y. J. Park, J. G. Kim, and M. K. Kim, *J. Power Sources*, **87**, 69 (2000).
3. M. Saitoh, M. Sano, M. Fujita, M. Sakata, M. Takata, and E. Nishibori, *J. Electrochem. Soc.*, **151**, A17 (2004).
4. S.-W. Lee, K.-S. Kim, H.-S. Moon, J.-P. Lee, H.-J. Kim, B.-W. Cho, W.-I. Cho, and J.-W. Park, *J. Power Sources*, **130**, 227 (2004).
5. Y. Matsuo, R. Kostecki, and F. McLarnon, *J. Electrochem. Soc.*, **148**, A687 (2001).
6. T. Inoue and M. Sano, *J. Electrochem. Soc.*, **145**, 3704 (1998).
7. J. Cho and M. M. Thackeray, *J. Electrochem. Soc.*, **146**, 3577 (1999).
8. Y.-K. Sun, *Electrochem. Commun.*, **2**, 6 (2000).
9. D. Song, H. Ikuta, T. Uchida, and M. Wakihara, *Solid State Ionics*, **117**, 151 (1999).
10. S.-C. Park, Y.-M. Kim, Y.-M. Kang, K.-T. Kim, P. S. Lee, and J.-Y. Lee, *J. Power Sources*, **103**, 86 (2001).
11. S.-W. Lee, K.-S. Kim, H.-S. Moon, H.-J. Kim, B.-W. Cho, W.-I. Cho, J.-B. Ju, and J.-W. Park, *J. Power Sources*, **126**, 150 (2004).
12. J. Cho, T.-J. Kim, and B. Park, *J. Electrochem. Soc.*, **149**, A288 (2002).
13. J.-S. Kim, C. S. Johnson, J. T. Vaugey, S. A. Hackney, K. A. Walz, W. A. Zeltner, M. A. Anderson, and M. M. Thackeray, *J. Electrochem. Soc.*, **151**, A1755 (2004).
14. N. J. Dudney, *J. Power Sources*, **89**, 176 (2000).